

# DC Spin Current Generation in a Rashba-type Quantum Channel

L. Y. Wang,<sup>1</sup> C. S. Tang,<sup>2</sup> and C. S. Chu<sup>1</sup>

<sup>1</sup>*Department of Electrophysics, National Chiao Tung University, Hsinchu 30010, Taiwan*

<sup>2</sup>*Physics Division, National Center for Theoretical Sciences, P.O. Box 2-131, Hsinchu 30013, Taiwan*

(Dated: September 29, 2018)

We propose and demonstrate theoretically that resonant inelastic scattering (RIS) can play an important role in dc spin current generation. The RIS makes it possible to generate dc spin current via a simple gate configuration: a single finger-gate that locates atop and orients transversely to a quantum channel in the presence of Rashba spin-orbit interaction. The ac biased finger-gate gives rise to a time-variation in the Rashba coupling parameter, which causes spin-resolved RIS, and subsequently contributes to the dc spin current. The spin current depends on both the static and the dynamic parts in the Rashba coupling parameter,  $\alpha_0$  and  $\alpha_1$ , respectively, and is proportional to  $\alpha_0\alpha_1^2$ . The proposed gate configuration has the added advantage that no dc charge current is generated. Our study also shows that the spin current generation can be enhanced significantly in a double finger-gate configuration.

PACS numbers: 73.23.-b, 72.25.Dc, 72.30.+q, 72.25.-b

Spintronics is important in both application and fundamental arenas [1, 2]. A recent key issue of great interest is the generation of dc spin current (SC) without charge current. Various dc SC generation schemes have been proposed, involving static magnetic field [3, 4], ferromagnetic material [5], or ac magnetic field [6]. More recently, Rashba-type spin-orbit interaction in 2DEG [7, 8] has inspired attractive proposals for nonmagnetic dc SC generation [9, 10, 11]. Of these recent proposals, including a time-modulated quantum dot with a static spin-orbit coupling [9], and time-modulations of a barrier and the spin-orbit coupling parameter in two spatially separated regions [10], the working principle is basically adiabatic quantum pumping. Hence simultaneous generation of both dc spin and charge current is the norm. The condition of zero dc charge current, however, is met only for some judicious choices for the values of the system parameters.

It is known, on the other hand, that quantum transport in narrow channel exhibits RIS features when it is acted upon by a spatially localized time-modulated potential [12, 13]. This RIS is coherent inelastic scattering, but with resonance at work, when the traversing electrons can make transitions to their subband threshold by emitting  $m\hbar\Omega$  [12, 13]. Should this RIS become spin-resolved in a Rashba-type quantum channel (RQC), of which its Rashba coupling parameter is time-modulated locally, we will have a simpler route to the nonmagnetic generation of dc SC. Thus we opt to study, in this Letter, the RIS features in a RQC. As is required by a study on the RIS features, our study goes beyond the adiabatic regime.

The system configuration considered is based on a RQC that forms out of a 2DEG in an asymmetric quantum well by the split-gate technique. As is depicted in Fig. 1(a), a finger gate (FG) is positioned above while it is separated from the RQC by an insulating layer. A local time-variation in the Rashba coupling parameter  $\alpha(\mathbf{r}, t)$  can be induced by ac biasing the FG [10, 11]. The

Hamiltonian is given by  $\mathcal{H} = p^2/2m + \mathcal{H}_{\text{so}}(\mathbf{r}, t) + V_c(y)$  where the Rashba term

$$\mathcal{H}_{\text{so}}(\mathbf{r}, t) = \mathbf{M} \cdot \frac{1}{2} [\alpha(\mathbf{r}, t)\mathbf{p} + \mathbf{p}\alpha(\mathbf{r}, t)]. \quad (1)$$

Here  $\mathbf{M} = \hat{z} \times \boldsymbol{\sigma}$ ,  $\hat{z}$  is normal to the 2DEG,  $\boldsymbol{\sigma}$  is the vector of Pauli spin matrices, and  $V_c(y)$  is the confinement potential. The unperturbed Rashba coupling parameter  $\alpha(\mathbf{r}, t)$  is  $\alpha_0$  throughout the RQC, but when perturbed by the ac biased FG, it becomes  $\alpha_0 + \alpha_1 \cos\Omega t$  in the region underneath the FG. The Dresselhaus term is neglected for the case of a narrow gap semiconductor system [14].

For a clear demonstration of the pumping mechanism, the unperturbed RQC we considered is narrow so that its subband energy spacing is much greater than the subband mixing due to the Rashba interaction. As such, the unperturbed Hamiltonian, in its dimensionless form, is  $\mathcal{H}_0 = -\nabla^2 + \alpha_0\sigma_y(i\partial/\partial x) + V_c(y)$ . Appropriate units have been used such that all physical quantities presented here, and henceforth, are dimensionless [13]. In particular,  $\alpha$  is in unit of  $v_F/2$ ,  $v_F$  denoting the Fermi velocity, and spin in unit of  $\hbar/2$ . The right-going (R) eigenstate of  $\mathcal{H}_0$ , in the  $n$ -th subband, is  $\phi_n(y)\psi_n^\sigma(x)$ , where  $\psi_n^\sigma(x) = \exp[ik_{n,R}^\sigma x]\chi_\sigma$ . The wavevector  $k_{n,R}^\sigma = \sqrt{\mu_n} + \eta_\sigma\alpha_0/2$

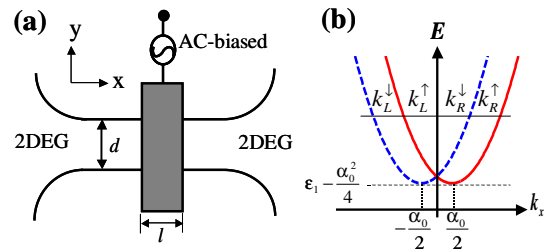


FIG. 1: (a) Top-view schematic illustration of the RQC. The ac-biased FG, of width  $l$ , is indicated by the grey area; (b) the electron dispersion relation of an unperturbed RQC.

while  $\eta_\sigma = \pm 1$  denotes the eigenvalue of  $\chi_\sigma$  to the operator  $\sigma_y$ .  $\mu_n$  is the energy measured from the  $n$ -th subband threshold such that the energy of the eigenstate is  $E = \mu_n + \varepsilon_n - \alpha_0^2/4$ , for  $\varepsilon_n = (n\pi/d)^2$ . This dispersion relation is shown in Fig. 1(b). It is of import to note, for later reference, that right-going electrons have  $|k_\uparrow^R| > |k_\downarrow^R|$ , and that at the subband threshold  $k_{\uparrow(\downarrow)}^R = k_{\uparrow(\downarrow)}^L$ .

In the ac-biased region,  $\mathcal{H} = \mathcal{H}_x + \mathcal{H}_y$ , the transverse part  $\mathcal{H}_y = -\partial^2/\partial y^2 + V_c(y)$ , and the longitudinal part

$$\mathcal{H}_x(t) = \left( -i\frac{\partial}{\partial x} + \frac{\alpha(x,t)}{2}\mathbf{M} \cdot \hat{\mathbf{x}} \right)^2 - \frac{1}{4}\alpha(x,t)^2. \quad (2)$$

The form of Eq. (2) suggests an effective vector potential,  $\mathbf{A}(t) = \frac{1}{2}\alpha(x,t)\mathbf{M} \cdot \hat{\mathbf{x}}$ , which depends on the spin and gives rise to a spin-resolved driving electric field  $\mathbf{E} = -\partial\mathbf{A}/\partial t$ . However, in  $\mathcal{H}_x$ , the  $A^2$  term does not depend on  $\sigma$ , while for the term linear in  $\mathbf{A}$ ,  $\mathbf{A} \chi_\sigma = -\frac{1}{2}\eta_\sigma \alpha(x,t) \chi_\sigma$  gives rise only to a trivial spin dependence, which can be easily removed by a shift in the origin of time for the case of an oscillatory  $\alpha(x,t)$ . Yet it turns out that the full term linear in  $\mathbf{A}$ , given by  $-i\frac{\partial}{\partial x} \hat{\mathbf{x}} \cdot \mathbf{A}$ , manages to give rise to nontrivial spin-resolved transmissions. In a perturbative sense, this term becomes  $k_{\uparrow(\downarrow)}^R A_x$ , for the case of a right-going electron incident upon a spatially uniform  $\alpha(t)$ . This renders the effective longitudinal driving field to become spin dependent. As a consequence, the difference in the current transmissions, for spin up and spin down cases, is proportional to  $\alpha_0$ , and the difference is found to be amplified by RIS. In a RQC that has zero source-drain bias, the spin-resolved current transmission leads readily to dc spin current, but it cannot lead to dc charge current if the RQC is symmetric with respect to its source and drain.

An alternate way to understand the origin of the spin-resolved current transmission is presented in the following. Performing a unitary transformation  $\Psi_\sigma(x,t) = \exp\left[(i\eta_\sigma/2) \int_{-l/2}^x \alpha(x',t) dx'\right] \psi_\sigma(x,t)$ , the Schrödinger equation, Eq. (2), becomes

$$\left[ -\frac{\partial^2}{\partial x^2} + U_1(t) + U_2^\sigma(t) \right] \psi_\sigma(x,t) = i\frac{\partial}{\partial t} \psi_\sigma(x,t), \quad (3)$$

of which the two time-dependent potentials are  $U_1(t) = -\alpha(x,t)^2/4$ , and  $U_2^\sigma(t) = (\Omega\alpha_1/2)(x+l/2)\cos(\Omega t + \eta_\sigma\pi/2)$ . Even though only  $U_2^\sigma$  depends on spin,

both the term in  $U_1(t)$  that oscillates with frequency  $\Omega$  and  $U_2^\sigma$  together constitute a pair of quantum pumping potential that pump SC. This is our major finding in this work: that spin pumping nature is build-in even in a single FG configuration. Its origin is rooted in the intricate Rashab spin dynamics.

The expression for the pumped SC, in the absence of the source-drain bias, is obtained from the SC density operator

$$\hat{j}_x^y = i \left[ \frac{\partial \Psi_\sigma^\dagger}{\partial x} \sigma_y \Psi_\sigma - \text{H. c.} \right] + \frac{\alpha}{2} \Psi_\sigma^\dagger \{ \sigma_y, \mathbf{M} \}_x \Psi_\sigma. \quad (4)$$

The SC conservation is maintained due to the suppression of subband mixing in a RQC, and the associated spin-flip mechanism. By taking the time-average of the transmitted and the incident SC in Eq. (4), and their ratio, we obtain the spin-resolved current transmission  $T_{\beta\alpha}^\sigma$ , where  $\alpha, \beta$ , are, respectively, the incident and the transmitting lead. Summing over all possible incident states from both reservoirs  $R$  and  $L$ , the net SC is given by

$$\begin{aligned} I^s &= I^\uparrow + I^\downarrow \\ &= \int dE f(E) \left[ (T_{RL}^\uparrow - T_{LR}^\uparrow) + (T_{LR}^\downarrow - T_{RL}^\downarrow) \right] \end{aligned} \quad (5)$$

where  $f(E)$  is the Fermi-Dirac distribution, and  $T_{RL}^\sigma = \sum_n \sum_{m(\mu_n^m > 0)} T_{n,RL}^{m,\sigma}$ . The transmission coefficient  $T_{n,RL}^{m,\sigma} = \left| t_{n,RL}^{m,\sigma} \right|^2 \sqrt{\mu_n^m/\mu_n}$  denotes the current transmission that an electron incident from terminal  $L$  in the spin channel  $\sigma$ , subband  $n$ , energy  $E$ , is scattered into terminal  $R$ , sideband  $m$ , with kinetic energy  $\mu_n^m = \mu_n + m\Omega$ . The net charge current is simply given by  $I^q = I^\uparrow - I^\downarrow$ . In a symmetric time-dependent FG configuration, we have  $T_{LR}^\sigma = T_{RL}^{-\sigma}$ , so that the net spin current is  $I^s = 2 \int dE f(E) (T_{RL}^\uparrow - T_{RL}^\downarrow)$  and the net charge current is identically zero.

Before we demonstrate numerically the robustness of the SC pumping, it is worthwhile to first look at the weak-pumping regime, which affords us analytical results. To this end, the scattering amplitudes are restricted to include only up to the sidebands  $m = \pm 1$ , that is, up to first power in  $\alpha_1$ . For an electron incident with wave vector  $k_{n,R}^\sigma$  from terminal  $L$ , the spin-resolved reflection amplitude is obtained to be

$$r_{n,LL}^{m,\sigma} = \eta_\sigma \left( \frac{\alpha_1}{2} \right) \frac{\left[ e^{i(k_{n,R}^\sigma - k_{n,L}^{m,\sigma})l} - 1 \right] \left[ \frac{1}{\Omega} k_{n,R}^\sigma \left( k_{n,R}^\sigma - k_{n,R}^{m,\sigma} \right) + \frac{m}{2} \right]}{k_{n,R}^{m,\sigma} - k_{n,L}^{m,\sigma}} \quad (6)$$

for  $m = \pm 1$ . The reflection amplitude  $r_{n,LL}^{0,\sigma}$  is of order  $\alpha_1^2$ , and is negligible in our weak-pumping approximation. Here the wave vector  $k_{n,R(L)}^{m,\sigma} = \pm(\mu_n^m)^{1/2} + \eta_\sigma \alpha_0/2$ , with upper (lower) sign corresponds to the right- (left-) moving electron in the  $n$ th subband,  $m$ th sideband, and with kinetic energy  $\mu_n^m$ . It is obvious then that differences between wave vectors of different sideband indices, but of the same spin state, are spin independent. Hence the spin dependence of  $r_{n,LL}^{\pm 1,\sigma}$  arises solely from the  $k_{n,R}^\sigma$  in the numerator that does not involve in a wave vector

difference. Furthermore, this spin dependence is associated with  $\alpha_0$ . It is not unexpected then that the SC is proportional to  $\alpha_0$ . The SC is related to the current transmission which, within the aforementioned approximation, is given by  $T_{RL}^\sigma \approx 1 - \sum_n [R_{n,LL}^{1,\sigma} + R_{n,LL}^{-1,\sigma}]$ , where  $R_{n,LL}^{m,\sigma} = |r_n^{m,\sigma}|^2 \sqrt{\mu_n^m}/\sqrt{\mu_n}$ . From Eq. (5), the energy derivative of the zero temperature SC is given by  $\partial I^s/\partial E = 2\Delta T_{RL} = 2(T_{RL}^\uparrow - T_{RL}^\downarrow)$  from which its explicit expression is given by

$$\frac{\partial I^s}{\partial E} = \frac{1}{2}\alpha_0\alpha_1^2 \sum_n \sum_{\substack{m=\pm 1 \\ (\mu_n^m > 0)}} \frac{[1 - \cos((\sqrt{\mu_n} + \sqrt{\mu_n^m})l)] \left[ \left(\frac{1}{4}\right)^2 - \left(\frac{1}{\Omega^2}(\mu_n + \sqrt{\mu_n\mu_n^m}) + \frac{m}{4}\right)^2 \right]}{\mu_n\sqrt{\mu_n^m}}. \quad (7)$$

That this expression diverges when  $\mu_n^m = 0$ , for  $m < 0$ , exhibits the RIS feature unambiguously.

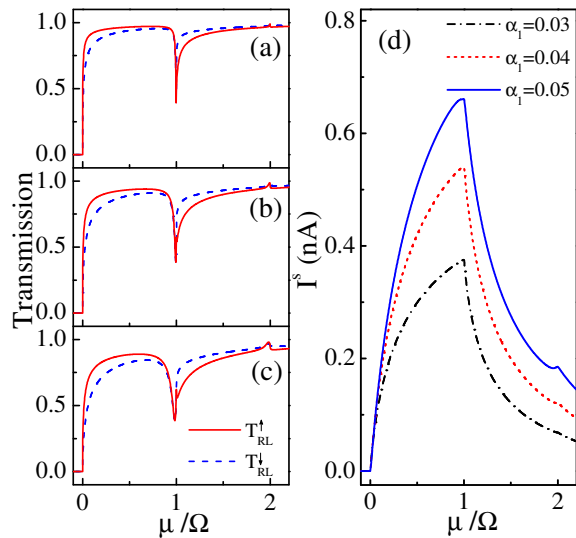


FIG. 2: Spin-resolved current transmissions  $T_{RL}^\uparrow$  (solid) and  $T_{RL}^\downarrow$  (dashed) versus the incident energy  $\mu/\Omega$ . Parameters  $N = 1$ ,  $\alpha_0 = 0.13$ ,  $\Omega = 0.002$ ,  $l = 20$ , and with  $\alpha_1 =$  (a) 0.03, (b) 0.04, and (c) 0.05. The corresponding dc SC is plotted in (d).

In the following, we present results obtained from solving the time-dependent spin-orbit scattering exactly, in the numerical sense [15]. Physical parameters are chosen to be consistent with the InGaAs-InAlAs based narrow gap heterostructures such that the electron density  $n_e = 1 \times 10^{12} \text{ cm}^{-2}$ , effective mass  $m^* = 0.04m_0$ , and  $\alpha_0 = 0.13$  ( $\hbar\alpha_0 = 3 \times 10^{-11} \text{ eV m}$ ) [8]. Accordingly, the length unit  $l^* = 4.0 \text{ nm}$ , and the energy unit  $E^* = 59$

meV.

For the case of one FG ( $N = 1$ ), the energy dependence of the spin-resolved transmission  $T_{RL}^\sigma$  is plotted in Figs. 2 (a)-(c), and that of the corresponding dc SC is plotted in Fig. 2 (d). The FG width  $l = 20$  (80 nm), driving frequency  $\Omega = 0.002$  ( $\nu = \Omega/2\pi \approx 28 \text{ GHz}$ ), and energy  $\mu = E - \varepsilon_1$ . Dip features in  $T_{RL}^\sigma$  at  $\mu/\Omega = 1$  are the QBS features, where electrons undergo coherent inelastic scattering to a QBS just beneath its subband bottom [12]. Higher order QBS features at  $\mu/\Omega = 2$  are barely shown by the small peaks. Of particular interest is the change in sign in the transmission difference  $\Delta T_{RL} = T_{RL}^\uparrow - T_{RL}^\downarrow$  across the dip structures, namely,  $\Delta T_{RL}(\mu = \Omega^-) > 0$  while  $\Delta T_{RL}(\mu = \Omega^+) < 0$ . This leads to a nonzero dc SC, and that it peaks at  $\mu/\Omega = 1$ , as is exhibited in Fig. 2(d). It is also shown that the dc SC increases with the oscillating amplitude  $\alpha_1$  of the ac-biased gate voltage.

The possibility of nonlinear enhancement in the dc SC by two FGs ( $N = 2$ ) is presented in Figs. 3 (a)-(c). The driving frequency is chosen to be  $\Omega = 0.001$  ( $\nu \approx 14 \text{ GHz}$ ), and the FG width  $l = 22$  ( $\approx 88 \text{ nm}$ ). For comparison, the  $N = 1$  FG transmissions are plotted along side with that of the  $N = 2$  FG case, in Figs. 3 (a), and (b), respectively. The corresponding dc SC, expressed in terms of pumped spin per cycle  $N_P^s = (2\pi/\Omega)|I_R^s|$ , is shown in Fig. 3(c). The pumping is optimized by a choice of the FG separation, with the edge to edge separation  $\Delta l = 22$ . That nonlinear effects are significant is supported by the appearance of up to the fourth-sideband QBS dip structures in Fig. 3(b). As indicated by arrows, the pumped spin per cycle peaks at  $\mu/\Omega \simeq 1.57$  (1.92), and with peak value 0.8 (0.1) for the case of  $N = 2$  ( $N = 1$ ) FG. The enhancement in  $N_P^s$  is nonlinear, far greater than doubling the  $N_P^s$  of  $N = 1$  FG.

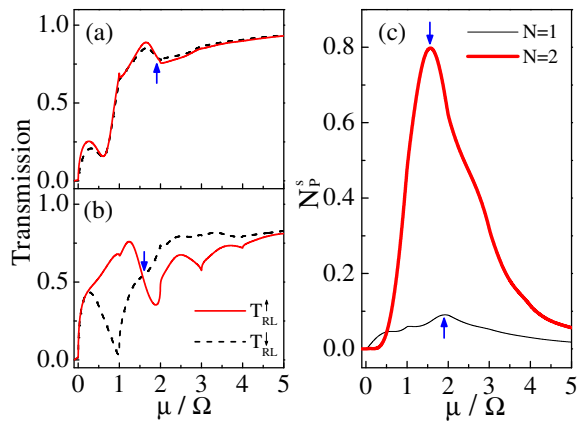


FIG. 3: Current transmission versus  $\mu/\Omega$  for  $N =$  (a) 1, and (b) 2. Pumped spins per cycle are plotted in (c) for  $N = 1$  (thick curve) and  $N = 2$  (thin curve) with driving frequency  $\Omega = 0.001$ . Other parameters are the same as in Fig. 2.

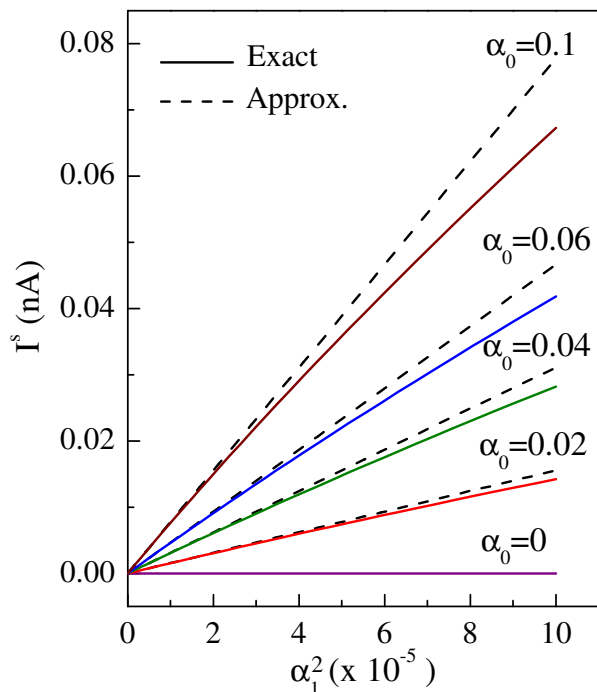


FIG. 4: Pumped dc SC versus  $\alpha_1^2$  for various  $\alpha_0$  values. Other parameters are  $\Omega = 0.01$  and  $l = 20$ .

In Fig. 4, we present the dependence of the dc SC peak values on the pumping parameters  $\alpha_0$  and  $\alpha_1$ , and for the case of one FG. The numerical results, depicted by solid curves, coincide nicely, in the small  $\alpha_1$  regime, with the one sideband approximation results, depicted by broken curves, and calculated according to Eq. (7). This confirms that the dc SC is proportional to  $\alpha_0\alpha_1^2$  in the weak pumping regime. Moreover, deviation of the numerical results from the weak pumping behavior sets in at smaller  $\alpha_1$  values when  $\alpha_0$  increases. Typical degree of deviation can be inferred from the case of  $\alpha_0 = 0.1$

and  $\alpha_1 = 0.01$ , where the deviation of dc SC  $\Delta I^s = |I_{\text{numerical}}^s - I_{\text{app}}^s|/I_{\text{numerical}}^s \simeq 0.16$ . We also find that, as  $\Omega$  decreases, the degree of deviation increases, indicating the need to include more sidebands for the description of the time-dependent quantum scattering.

In conclusion, a nonmagnetic way of generating dc SC has been established. The proposed configuration, a Rashba-type quantum channel driven by an ac biasing finger gate, is relatively simple and is within reach of recent fabrication capability. The nature of the spin pumping is studied in detail and its pumping mechanism understood. Resonant inelastic process is found to be a major factor that contributes to the robustness of the spin pumping. The coherent nature of the pumping supports further enhancement of the spin pumping by invoking configuration consisting of more than one finger gates.

The authors acknowledge valuable discussions with A. G. Mal'shukov. This work was funded by the National Science Council of ROC under Grant Nos. NSC92-2112-M-009-035, NSC92-2120-M-009-010, NSC93-2112-M-009-036 and NSC93-2119-M-007-002 (NCTS).

- 
- [1] *Semiconductor Spintronics and Quantum Computation*, edited by D.D. Awschalom, N. Samarth, and D. Loss (Springer-Verlag, Berlin, 2002).
  - [2] S.A. Wolf *et al.*, *Science* **294**, 1488 (2001); Y. Kato *et al.*, *ibid.* **299**, 1201 (2003); S. Murakami *et al.*, *ibid.* **301**, 1348 (2003).
  - [3] E. R. Mucciolo, C. Chamon, and C. M. Marcus, *Phys. Rev. Lett.* **89**, 146802 (2002). Experimental realization was reported by S. K. Watson, R. M. Potok, C. M. Marcus, and V. Umansky in *Phys. Rev. Lett.* **91**, 258301 (2003).
  - [4] Q. F. Sun, H. Guo, and J. Wang, *Phys. Rev. Lett.* **90**, 258301 (2003).
  - [5] A. Brataas, Y. Tserkovnyak, G. E. W. Bauer, and B. I. Halperin, *Phys. Rev. B* **66** 60404 (2002).
  - [6] P. Zhang, Q. K. Xue, and X. C. Xie, *Phys. Rev. Lett.* **91**, 196602 (2003).
  - [7] Y. A. Bychkov and E. I. Rashba, *J. Phys. C* **17**, 6039 (1984).
  - [8] J. Nitta *et al.*, *Phys. Rev. Lett.* **78**, 1335 (1997); D. Grundler, *ibid.* **84**, 6074 (2000).
  - [9] P. Sharma and P. W. Brouwer, *Phys. Rev. Lett.* **91**, 166801 (2003).
  - [10] M. Governale, F. Taddei, and R. Fazio, *Phys. Rev. B* **68**, 155324 (2003).
  - [11] A. G. Mal'shukov, C. S. Tang, C. S. Chu, and K. A. Chao, *Phys. Rev. B* **68**, 23 3307 (2003).
  - [12] P. F. Bagwell and R. K. Lake, *Phys. Rev. B* **46**, 15329 (1992).
  - [13] C. S. Tang and C. S. Chu, *Phys. Rev. B* **53**, 4838 (1996).
  - [14] G. Lommer, F. Malcher, and U. Rössler, *Phys. Rev. Lett.* **60**, 728 (1988).
  - [15] L. Y. Wang, C. S. Tang, and C. S. Chu (unpublished).